JOURNAL OF CATALYSIS **163,** 338–345 (1996)
ARTICLE NO. 0335

Studies on Pt_xIn_y Bimetallics in NaY

II. Further Characterization Results and Catalytic Properties

P. Mériaudeau,[1] A. Thangaraj, J. F. Dutel, P. Gelin,[2] and C. Naccache

Institut de Recherches sur la Catalyse—CNRS, 2 av. A. Einstein, 69626 Villeurbanne, France

Received November 27, 1995; revised June 10, 1996; accepted June 11, 1996

In a previous paper the preparation and the characterization of PtNaY and PtInNaY were reported. Here, complementary characterization results obtained by studying the TPD of CO by mass spectrometry coupled with IR studies of the adsorbed CO phases indicated no apparent change in the electronic properties of Pt. Comparison of catalytic properties for *n*-butane hydrogenolysis between PtNaY and PtInNaY indicated that the hydrogenolysis is deeply affected by the addition of In to Pt; the kinetic parameters (apparent activation energy, relative order for butane and for hydrogen) are modified by In addition. These results are explained considering that In is acting more like a diluent of Pt atoms than as an electronic modifier of Pt.

INTRODUCTION

The discovery that bimetallic catalysts exhibited better catalytic performance in hydrocarbon dehydrogenation or in reforming reaction has led to a considerable number of investigations aimed at describing the effect of the addition of nonactive metal atoms into active metal. In particular, the literature relative to platinum alloyed with a nonactive metal like Sn is well documented. It is well known and relatively well explained how the addition of Sn to Pt imparts to platinum catalysts large improvement in selectivity and stability for reforming and dehydrogenation reactions. By contrast there are few reports devoted to the study of platinum–indium bimetallic catalysts which have been cited as interesting materials for dehydrogenation (1).

In a recent issue of this journal, we described the preparation and the characterization of PtIn bimetallics in NaY hosts (2). From this study, it has been concluded that small PtIn particles (1–2 nm) are formed inside the cavities of NaY. From X-ray photoelectron spectroscopy (XPS) measurements and IR spectra of adsorbed CO it was established that Pt and In are at zero valence state, no evidence for change in the Pt electronic state being observed. For all the In loadings, it has been observed that only part of In is alloyed with Pt, the other part remaining as In^{3+} either in the form of well dispersed In_2O_3 or in the form of In^{3+} in an ionic exchange position. In this paper, we will report further characterization of Pt and PtIn in NaY and their catalytic properties for butane hydrogenolysis. The hydrogenolysis of *n*-butane has been preferred to the reaction of propane because it will provide us data on the effect of alloying Pt with In on the activation of terminal and internal carbon–carbon bond.

EXPERIMENTAL

Preparation of the Catalysts

The catalysts were fully described in (2). We will briefly summarize the most important points.

Samples were prepared using NaY zeolite coexchanged with Pt^{2+} and In^{3+}. Pt loading was 5 wt% and In loading was in the range 0 to 5 wt%, labeled as Pt_5 and In_xNaY, respectively. Before characterization, the samples were first oxidized under a flow of O_2, the temperature being increased from RT to 593 K (ramping, 0.2 K/min), and after 2 h at 593 K, O_2 was replaced with N_2 and the sample was reduced under a flow of H_2, the temperature being increased from 593 to 773 K (0.5 K/min). After 2 h at 773 K, H_2 was flushed with N_2 and the sample was cooled down to RT before allowing contact with air.

CO Chemisorption and Desorption Studies

The samples were pressed into thin wafers (15 mg, 18 mm diameter) and mounted into IR cells as described earlier (3), allowing *in situ* observation at different temperatures. In order to ensure a proper heat transfer through the pellet, the wafer was mounted onto the sample holder together with a CaF_2 plate of the same size as the sample wafer.

The temperature was measured by a thermocouple inserted between the sample holder and the CaF_2 plate. The sample was heated by a home-built temperature controller

[1] To whom correspondence should be addressed.

[2] Present address: LACE, Université Clde Bernard, 43 bd 11 nov, 69626 Villeurbanne, France.

0021-9517/96 $18.00

allowing linear temperature ramping. The reproducibility of the temperature programmed desorption (TPD) experiments is better than 5 K. The IR cell was connected to a stainless steel UVH system allowing for a vacuum of $>1.3 \times 10^{-4}$ Pa, equipped with a mass spectrometer allowing measurement of the gas phase composition (LEYBOLD Inficon Quadrex 20). Infrared spectra were measured on a Brucker IFS-48 FT-IR spectrometer.

Experimental Procedure for the IR-TPD Measurements

The sample wafer in the IR cell was outgassed for 16 h at RT and then heated to 573 K (3 K/min) and outgassed for 3 h. Then sample was contacted with 0.66 kPa of H_2, and the temperature was raised to 773 K (10 K/min). After 4 h at this temperature, the gas phase was removed and the sample cooled to RT. CO (0.6 kPa) was added to the IR cell; after 10 min, the CO gas phase was removed and the TPD study performed. The sample was heated at 5 K/min from RT to 773 K, the mass number 28 being continuously recorded by mass spectrometry; simultaneously the IR spectra were recorded with a sequence of 2 min. The registration of each IR spectrum is performed in 10 s, which corresponds to a temperature increase of 0.8 K. A blank experiment was systematically performed following each TPD and IR experiment in order to determine the response of the cell and correct the baselines. CO gas (99.99% purity) was from Air Liquide and was purified by passage through a molecular sieve unit.

Catalytic Measurements

The reaction of *n*-butane (Air Liquide, 99.99% purity) was studied in the temperature range of 573–673 K. A microreactor operating at atmospheric pressure and in a differential mode was employed. Low conversion was maintained over the sample by adequate adjustment of the contact time. We made sure that the rates measured were independent of the contact time. Pt_5 and Pt_5In_xNaY samples deactivate with time on stream. In order to obtain reliable results over the different samples, the bracketing technique was used in order to avoid significant deactivation.

For this purpose, the sample was reacted with *n*-butane + H_2 for 3 min and then flushed with H_2 for 20 min. This procedure allowed us to maintain the catalytic activity of the sample constant when the experimental conditions of the reaction were kept identical. The analysis of the reactant and products was performed at the end of each 3-min run. H_2 and N_2 (from Air Liquide, 99.99% purity) were purified by passage through a Deoxo unit and a molecular sieve unit.

RESULTS AND DISCUSSION

TPD of CO

The TPD profiles derived from mass number 28 peak intensity for CO adsorbed on Pt_5NaY and $Pt_5In_{3.1}NaY$ are shown, respectively, on Figs. 1a and 1b. Figure 1a indicates that the number of adsorbed CO molecules is larger for Pt sample compared to PtIn, the ratio being close to 2, in good agreement with measurements reported earlier for the Pt_5NaY sample (the Pt dispersion, as measured by H_2 chemisorption is 0.98, compared to 0.50 for $Pt_5In_{3.1}NaY$ (2)). The TPD profile obtained for PtNaY is characterized essentially by two peaks, one having a maximum close to 423 K, and the other being much broader, ranging between 473 and 673 K. For $Pt_5In_{3.1}NaY$, the TPD profile is much smoother but the temperature profile occurs in the same range as for Pt_5NaY, in particular for CO species desorbing at high temperatures. From these data it appears that the ratio (number of CO molecules desorbing at $T \leq 473$ K/total number of adsorbed CO molecules) is larger for Pt_5NaY than for $Pt_5In_{3.1}NaY$.

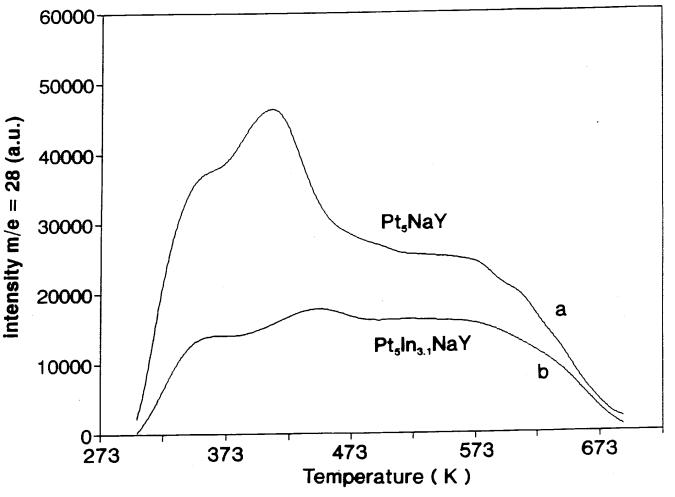

FIG. 1. TPD of CO adsorbed on Pt_5NaY (a) and $Pt_5In_{3.1}NaY$ (b).

IR Spectroscopy Results

Figures 2 and 3 show the IR spectra of adsorbed CO on Pt_5NaY and $Pt_5In_{3.1}NaY$, respectively, and their change as a function of the temperature of desorption.

As reported in (2) the spectrum of CO adsorbed on Pt_5NaY at 293 K and at full CO coverage exhibited a strong carbon monoxide stretching frequency centered at 2080 cm^{-1} and a weak shoulder at 2000 cm^{-1}. In addition weak IR bands at 1855 and 1800 cm^{-1} are visible. The IR band at 2080 cm^{-1} is attributed to Pt–CO linear singleton and the vibrations at 1855 and 1800 cm^{-1} to bridged or triply bonded CO (4). Two distincts features were observed in the IR spectrum of CO adsorbed on $Pt_5In_{3.1}NaY$: the IR bands of multiply bonded CO at 1855 and 1800 cm^{-1} are absent and the stretching frequency of linearly bonded CO shifted to a lower wavenumber. These two observations were considered as indirect evidence that in PtIn samples, Pt and In formed a bimetallic molecule in which Pt atoms are diluted

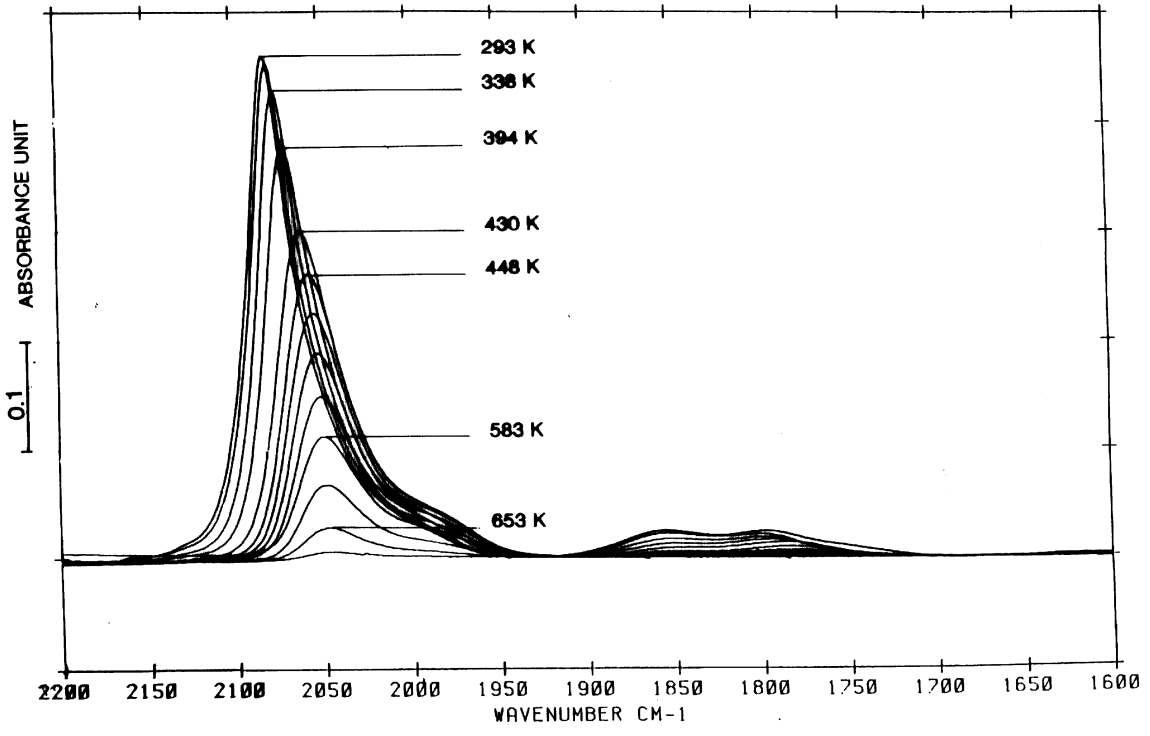

FIG. 2. IR spectra of adsorbed CO on Pt_5NaY. Change as a function the desorption temperature.

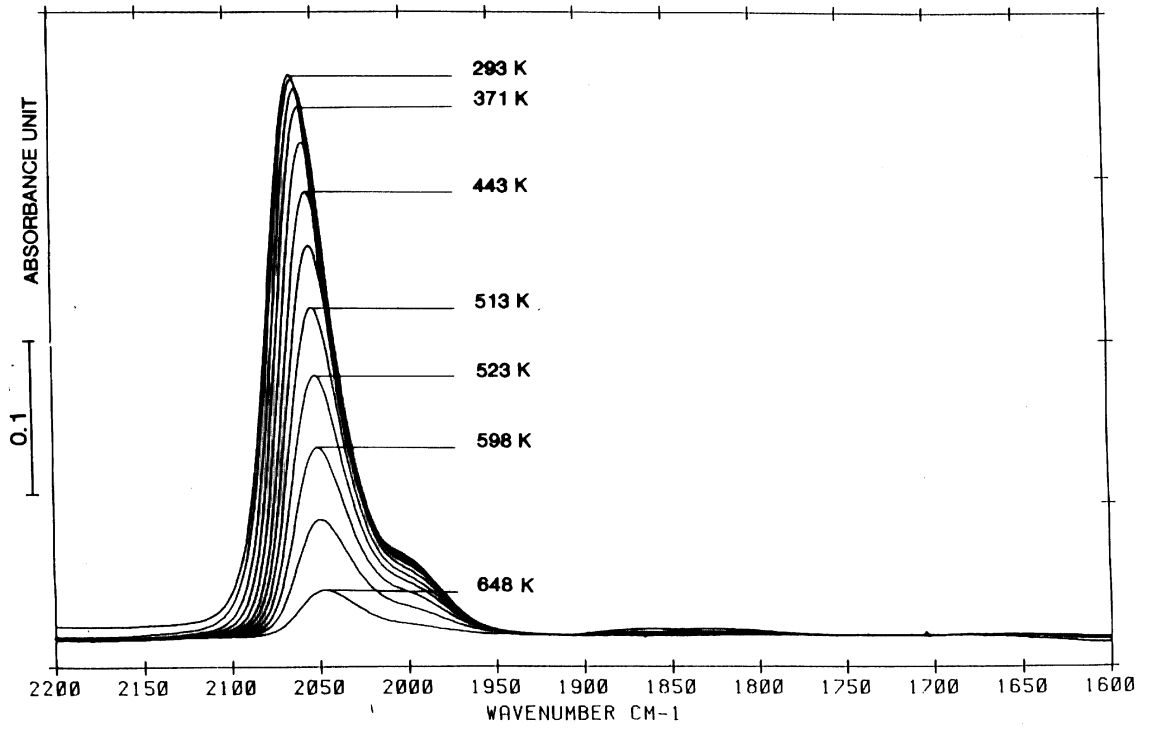

FIG. 3. IR spectra of adsorbed CO on $Pt_5In_{3.1}NaY$. Change as a function the desorption temperature.

by In atoms (2). The desorption of CO on Pt_5NaY with increasing temperature caused a decrease of both linear and bridged CO species, the decrease being larger for bridged CO species than for linear species. Above 523 K, the bridged CO were completely removed while the linear CO species were still observed. These features appear more clearly in Figs. 4 and 5 where the change in the absorbance of both linear and birdged CO species has been plotted as a function of the desorption temperature.

On Fig. 4, the rate of disappearance of linear (■) and bridged (□) species has been plotted as a function of the desorption temperature: so the experimental point corresponding to desorption temperature T_0 has been obtained by substracting from the IR spectrum obtained at T_0, the spectrum obtained at $T_0 - 2$ K; the variation of the linear CO species has been obtained by considering the integrated intensity of the CO adsorption between 2150 and 1920 cm^{-1} and that of bridged CO species by considering the adsorption between 1920 and 1700 cm^{-1}. On the same figure, the TPD spectrum of CO desorption, as obtained by mass spectrometry, has been reported for comparison. The same treatment of the data represented on Fig. 3 was performed for the $Pt_5In_{3.1}NaY$ sample, results shown in Fig. 5. If it is accepted that all the CO disappearing from the adsorbed as phase is appearing in the gas phase (no carbon deposit on the solid), it is expected that the temperature profile for the TPD of CO as obtained by mass spectrometry and that calculated from the IR spectra registered at increasing temperature would be the same. The maximum in desorption, as measured from IR experiments coincides exactly with the maximum observed on the TPD profile from gas phase analysis.

For the $Pt_5In_{3.1}NaY$ sample, increasing the temperature of CO desorption results in a progressive removal of CO

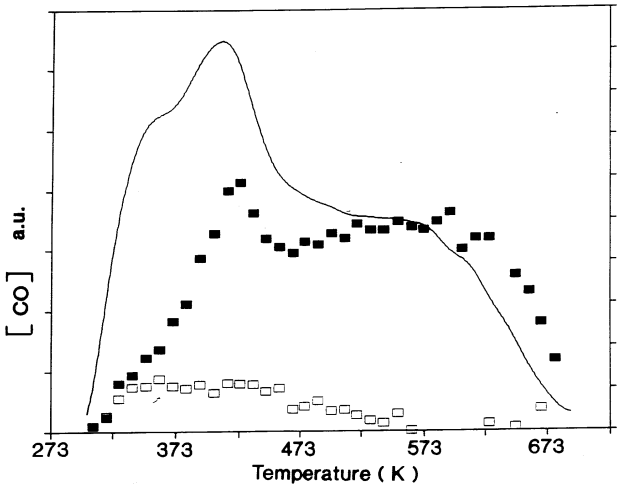

FIG. 4. Adsorption of CO on Pt_5NaY—comparison between TPD of CO (mass spect., solid line) and TPD of CO as calculated with IR spectra (■, Pt–CO singleton; □, bridged CO species).

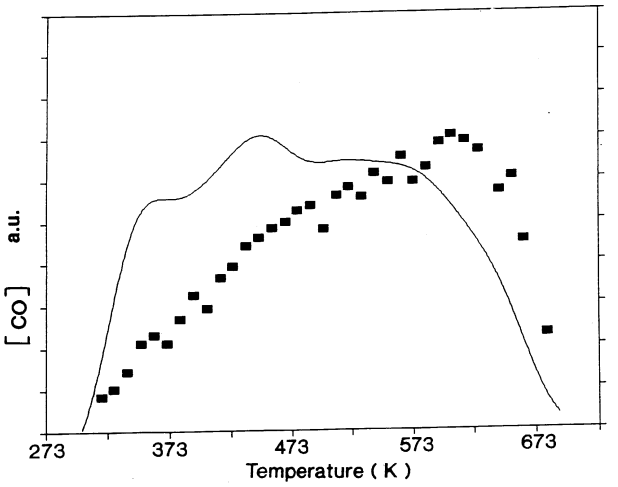

FIG. 5. Adsorption of CO on $Pt_5In_{3.1}NaY$—comparison between TPD of CO (mass spect., solid line) and TPD of CO as calculated with IR spectra (■, Pt–CO singleton).

species, as shown in Fig. 5. Comparison between results obtained by mass spectrometer and IR spectroscopy (Figs. 4 and 5) indicated that for high temperatures ($T > 573$ K) the TPD profiles do not have the same shape. This feature could be due to a change of the extinction coefficient of νCO vibration when T is increased; the higher the T, the higher the extinction coefficient. The analysis of the TPD profile obtained by mass spectrometry indicates that the relative number of CO molecules desorbing at $T \leq 473$ K is higher for Pt_5NaY than for $Pt_5In_{3.1}NaY$. This could be due (at least partially) to the fact that on the $Pt_5In_{3.1}NaY$ sample there are only few bridged CO species which are desorbing at $T \leq 473$ K and by contrast, on the Pt_5NaY sample, the bridged Co species are contributing significantly to the whole TPD spectrum.

Figure 6 shows the change of νCO as a function of the temperature for Pt_5NaY and $Pt_5In_{3.1}NaY$. It is observed that when the temperature is increased, the population of adsorbed CO decreases, and νCO decreased to the same value for both the samples ($\nu CO \rightarrow 2045$ cm^{-1} when CO coverage $\rightarrow 0$). This observation, assuming that the metal particle sizes were almost identical in Pt_5NaY and $Pt_5In_{3.1}NaY$ indicates that the electronic properties of Pt, as far as they are related to the CO adsorption, are not much modified by the addition of indium. This result is in agreement with previous conclusions (2). Figure 6 also indicates that the νCO shift, as a function of the desorption temperature (or of CO coverage) is larger for Pt_5NaY than for $Pt_5In_{3.1}NaY$; since the νCO shift as a function of the CO coverage is due to the weakening of the dipolar interaction between the adsorbed CO molecules, this indicates that for $Pt_5In_{3.1}NaY$, CO vibrators are well separated from each other, even at high coverage, probably because In atoms are diluting Pt atoms. Another possible explanation for this phenomenon (same

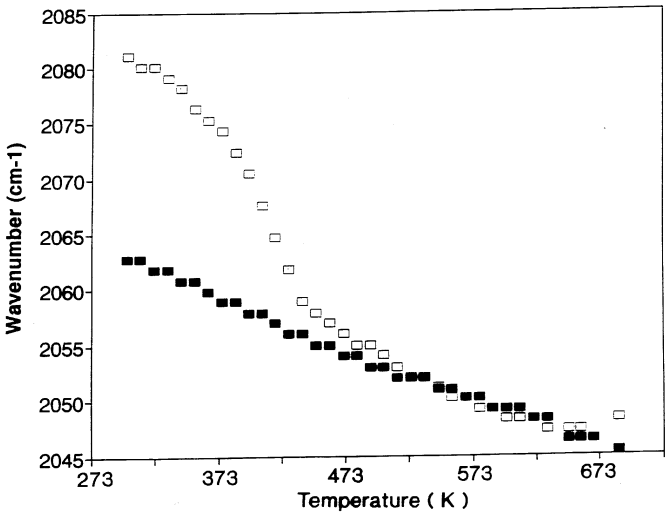

FIG. 6. Adsorption of CO on Pt_5NaY (□) and on $Pt_5In_{3.1}NaY$ (■). Change of νCO versus temperature of desorption.

value for νCO for CO coverage extrapolated to zero), is that if the bimetallic molecule is not homogeneously formed (some Pt particles do not contain In) and if CO is more weakly adsorbed on In modified Pt than on unmodified Pt, then CO would desorb first from modified Pt and remain adsorbed on the unmodified Pt, and by consequence, on the two solids, Pt_5NaY and P $Pt_5In_{3.1}NaY$, νCO will reach the same value at low CO coverages.

Examination of Fig. 6 indicates that νCO is the same on both solids when the desorption temperature reaches 500 K.

By using the TPD curves represented on Fig. 1, one can calculate that for the Pt_5NaY sample, at $T = 500$ K, the CO coverage is one-third of the initial CO coverage which was assumed to be 1 (2); for the $Pt_5In_{3.1}NaY$ sample the remaining CO coverage is at 500 K, one-half of the initial coverage. Thus, the above hypothesis is not compatible with the TPD results. Moreover, the examination of Figs. 2 and 3 clearly indicate that if there are some unalloyed Pt particles in $Pt_5In_{3.1}NaY$ sample, there are only few since bridged CO species are strongly depressed by In addition.

CATALYTIC RESULTS

Table 1 lists the kinetic parameters for the reaction. The bracketing technique (see Experimental) allowed us to obtain reproducible experimental values for the rates of reaction when the reaction temperature was varied back and forth, as shown in Table 1. The conversion of butane was kept low to allow true kinetic parameter determination.

The butane pressure was varied in the range 2.6–14 kPa, the H_2 pressure was fixed to 78.5 kPa, and the H_2 pressure was varied in the range 39–91 kPa, butane pressure being fixed at 9.3 kPa. The results are shown in Figs. 7–10. At first glance, Table 1 indicates clearly that the catalytic properties of Pt in *n*-butane reaction were considerably modified by the addition of indium. Not only was the rate of reaction substantially decreased by adding In but so was the activation energy and the kinetic parameters. The monometallic Pt catalyst is the most active. On the $Pt_5In_{3.1}NaY$ sample the rate of butane hydrogenolysis decreases drastically; the TOF is decreased by a factor of 16 for the $Pt_5In_{3.1}NaY$ sample. Simultaneously, the activation energy increased from 100 kJ/mol up to 142 kJ/mol.

There are numerous reports in the literature relative to the hydrogenolysis of *n*-butane on Pt catalysts (5–7 and references therein). The reaction was found very sensitive to self-poisoning (8) and to experimental conditions and this could explain the broad range of kinetic parameters: with Pt supported samples, different Pt loadings, and different supports (SiO_2, Al_2O_3) the relative hydrogen order measured in similar experimental conditions was found to be

TABLE 1

***n*-Butane Hydrogenolysis over Pt and PtInNaY Samples**

Catalyst	r_1[a]	E_A[b]	O_H[c]	O_B[c]	S_{C_2}[d]	S_{C_1}[e]	$\sqrt{i}/\sqrt{H}$[f]	TON[g] (h^{-1})	α%[h]
Pt_5NaY	11.5	100	0.5	0	26	20	0.22	46	2.1 [2.0]
Pt_5In_1NaY	4	108	0	0.30	19	22	0.18	18.6	1.1 [1.1]
$Pt_5In_{3.1}NaY$	0.35	142	−0.83	0.85	20	20	0.23	2.8	0.4 [0.4]

Note. $P_{C_4H_{10}} = 8.6$ kPa, $P_{H_2} = 92.4$ kPa. $T = 625$ K. Time on stream, 3 min. α, conversion.

[a] Rate of butane hydrogenolysis in mmol h^{-1} g^{-1} catalyst.

[b] E_A, apparent activation energy, kJ/mol.

[c] O_H, order relative to hydrogen; O_B, order relative to butane.

[d] Selectivity into ethane.

[e] Selectivity into methane.

[f] Ratio of the rate of isomerisation of *n*-butane into isobutane, by the rate of hydrogenolysis. This ratio is only indicative because in the butane feed, the iC_4 impurity renders difficult accurate measurement of isobutane formation.

[g] Calculated by using Pt dispersions as reported in (2).

[h] *n*-Butane conversion. Values in brackets have been obtained after having varied the temperature for measuring the apparent activation energy.

equal to 0.4 (7) ($P_{HC} = 10$ kPa, 90.9 kPa $\geq P_{H_2} \geq$ 50.5 kPa) to 0 (8) ($P_{HC} = 7.1$ kPa, 90.9 kPa $\geq P_{H_2} \geq$ 40.4 kPa) or to -0.4 (9) ($P_{HC} = 4$ kPa, 90.9 kPa $\geq P_{H_2} \geq$ 58.6 kPa). These findings suggest that either the Pt particle size, which was different in these studies, is a major parameter and/or that the kinetic measurements were performed on more or less partially deactivated samples.

In this work, due to the experimental procedure employed, it is expected that the results listed in Table 1 are representative of clean surfaces and are close to those reported in (7).

The addition of indium decreases the rate of butane hydrogenolysis without drastically changing the distribution of the products, suggesting that the addition of In to Pt changes the number of active sites more than it changes their nature.

In line with this suggestion are the results showing the distribution of the hydrogenolysis products as a function of the reaction temperature (Fig. 7) or as a function of the hydrogen pressure (Fig. 8). The same trend for butane hydrogenolysis was observed over PtNaY and PtInNaY samples. The selectivity of these catalysts toward the formation of ethane increased as the reaction temperature increased. Furthermore, over these catalysts, the ratio of the rate of C_3/rate of C_1 is always less than 1 and decreased as the reaction temperature increased. These observations suggest strongly that C_3, which was formed by the hydrogenolysis reaction $C_4 \rightarrow C_3 + C_1$, is further transformed into $C_2 + C_1$ even at the lowest reaction temperature used in this work. These results are in agreement with those reported by Paffett *et al.* (6). On the same figures the ratio of the rate of C_2/rate of C_1 is plotted as a function of the temperature; it appears that this ratio increases when the temperature is

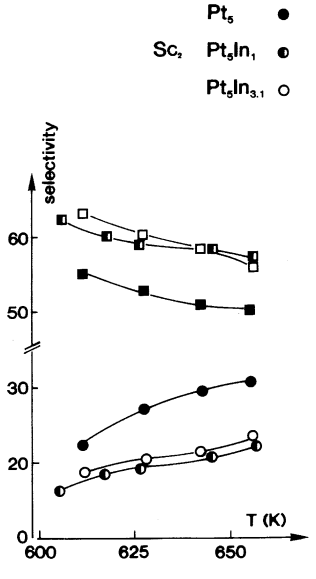

FIG. 7. Hydrogenolysis of *n*-butane. Change in the product distribution as a function of the reaction temperature.

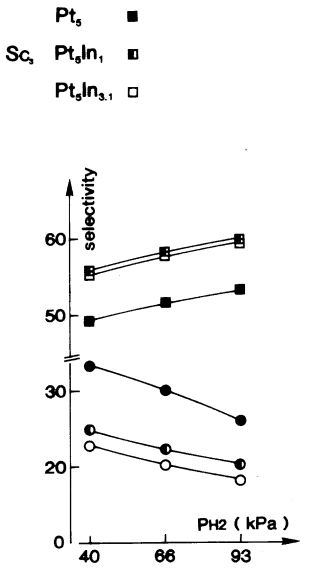

FIG. 8. Hydrogenolysis of *n*-butane. Products distribution as a function of the hydrogen pressure.

increased. It may also be that at higher temperatures, secondary hydrogenolysis of propane and ethane occurs with the subsequent formation of additional methane. However, since the data were obtained at low or very low butane conversions this hypothesis has not been further considered. This result suggests that the butane hydrogenolysis is occurring via

$$C_4H_{10} + H_2 \rightarrow CH_4 + C_3H_8 \quad [1]$$

$$C_4H_{10} + H_2 \rightarrow 2C_2H_6, \quad [2]$$

reaction [2] being favored at high temperatures. This explanation is in agreement with previous work on Pt/Al_2O_3 (5) in which it has been shown that the apparent activation energy is 159 kJ mol for C_2 formation via reaction (b) and 125 kJ/mol for C_3 formation via reaction [1].

Comparison of the slopes of rate of C_2/rate of C_1 and rate of C_3/rate of C_1 indicated that two phenonema are occuring when T is increased:

—Eq. [2] is favored

—Eq. [1] has to be modified because a deeper hydrogenolysis is favored.

In line with this conclusion are the results reported in Figs. 9 and 10 indicating that the selectivity is also a function of the hydrogen pressure. The ratio of the rate of C_3/rate of C_1 is not much modified with P_{H_2} but is always lower than 1.

By contrast the ratio of the rate of C_2/rate of C_1 increased as the hydrogen pressure decreased, which indicates that for low surface coverage with hydrogen the *n*-butane is preferentially adsorbed via carbon atoms at positions 2 and 3 in the chain, which results in the preferential C(2)–C(3) bond splitting.

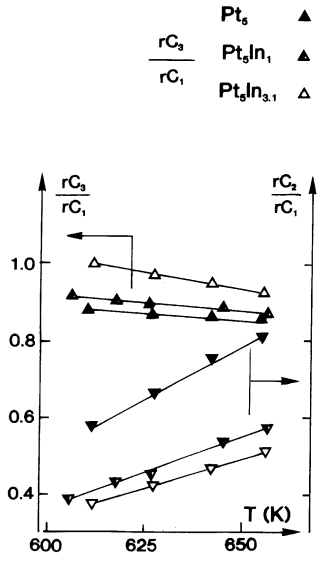

FIG. 9. Hydrogenolysis of *n*-butane. Rate of C_3/rate of C_1, rate of C_2/rate of $C_1 = f(T)$.

For the same P_{H_2}, the ratio of the rate of C_2/rate of C_1 is much less over PtIn samples than over pure Pt sample.

Dilution of Pt with indium apparently produced the same effect on the hydrogenolysis on *n*-butane in the C(2)–C(3) bond as the increase of the Pt surface coverage with H_2. The similarity of the In addition and of the coverage of Pt atoms with hydrogen on the C(2)–C(3) bond splitting is more in favor of a dilution effect than of an electronic effect when Pt is alloyed with In. Independently of the hydrogen pressure or of the reaction temperature, the ratio of the rate of C_3/rate of C_1 is larger for PtIn samples that for Pt sample, indicating

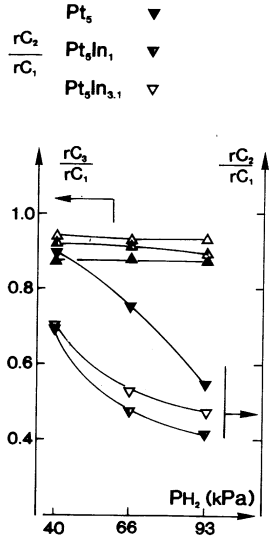

FIG. 10. Hydrogenolysis of *n*-butane. Rate of C_3/rate of C_1, rate of C_2/rate of $C_1 = f(P_{H_2})$.

that the deep hydrogenolysis transforming C_3H_x fragments into methane is less favorable by the indium addition. This trend is similar to that reported in (10) for Pt/Al_2O_3 or in (6) for $p(2 \times 2)$ Sn Pt(111) surface alloy samples for which the change in the hydrogenolysis product distribution was monitored as a function of the coking. Thus, a rough estimate suggests that In is acting mainly through a geometric effect. The value of the apparent activation energy obtained for Pt_5NaY is close to those reported in (7) and (11) for Pt/SiO_2 or for Pt(111) (12).

The increase in the apparent activation energy (Table 1) observed for Pt_5In_1 and $Pt_5In_{3.1}NaY$ samples compared to Pt_5NaY is rather difficult to discuss because it is known that for Pt/Al_2O_3 the apparent activation energy is changing with the amount of coking and with the Pt loading (10) or for Pt/C with the preparation of the solid (13). If one assumes that, due to our experimental procedure, the surfaces are clean, this result suggest that kinetic parameters which have been modified through the indium addition are involved in the determination of the activation energy.

Recently Cortright and Dumesic (14) have shown by microcalorimetry measurements that the heat of adsorption of C_2H_4 is lower for $PtSn/SiO_2$ than for Pt/SiO_2: with the initial heat of ethylene adsorption there is a decrease of 35 kJ/mol when Pt is alloyed with Sn (1 : 1.5 Pt/Sn). It has been suggested that the addition of tin inhibits the formation of highly dehydrogenated surface species. In agreement these results are the reports of Xu *et al.* (15) who showed by TPD measurements on Pt(111) and Sn/Pt(111) that the activation energy for desorption of butane decreased by 5–8 kJ/mol by adding tin to Pt surface. Preliminary results obtained in our laboratory by microcalorimetry on PtNaY and PtInNaY samples have shown similar behavior (16): a decrease of 20 kJ/mol was observed between the initial heat of adsorption of *n*-butane on Pt_5NaY and on $Pt_5In_{3.1}NaY$.

Thus, it appears that the strength of the interaction between platinum and hydrocarbon molecules like butane is lowered with the addition of an element like Sn or In to Pt; this weaker adsorbate surface bonding has been related to the electronic influence of Sn on Pt properties (15). Indeed, in the same experimental conditions, the hydrocarbon and H_2 coverages should be different for PtSn (or PtIn) and Pt samples and this could induce a change in the apparent activation energy.

CONCLUSIONS

In the part I of this work, it has been shown that PtIn bimetallics were formed in NaY hosts. The results in CO adsorption using TPD experiments and IR spectroscopy have shown that Pt–CO bonding is not much modified for PtInNaY compared to PtNaY; the $Pt_5In_{3.1}NaY$ sample contains more Pt sites having a larger Pt–CO bond strength than pure the Pt sample but the range of energies is the same.

IR results indicated that as $\theta CO \rightarrow 0$, νCO (singleton vibrator) is the same for monometallic or bimetallic samples, suggesting that the electronic modifications of Pt due to In addition are not large. Hydrogenolysis of butane has shown that the addition of indium decreased the number of active sites; the kinetic parameters of the reaction are different for both the samples and this could be the major effect explaining the change observed for the apparent activation energies.

REFERENCES

1. U.S. Patent 4,822,942 to Mobil.
2. Meriaudeau, P., Naccache, C., Thangaraj, A., Bianchi, C. L., Carli, R., and Narayanan, S., *J. Catal.* **152**, 313 (1995).
3. Echoufi, N., and Gelin, P., *J. Chem. Soc. Faraday Trans. I* **88**, 1067 (1992).
4. Toolenaar, F. J. C., Stoop, F., and Ponec, V., *J. Catal.* **82**, 1 (1983).
5. Leclercq, G., Leclercq, L., and Maurel, R., *J. Catal.* **44**, 68 (1976).
6. Szanyi, S., Anderson, S., and Paffett, M. T., *J. Catal.* **149**, 438 (1994).
7. Leclercq, G., El Gharbi, A., and Pietrzyk, S., *J. Catal.* **144**, 118 (1993).
8. Bond, G. C., Cunningham, R. M., and Short, E. L., *in* "Proceedings, 10th International Congress on Catalysis, Budapest 1992" (L. Guczi, F. Solymosi, and P. Tetenyi, Eds.). Akadémiai Kiadó, Budapest 1993.
9. Bond, G. C., and Yide, X., *J. Chem. Soc. Faraday Trans. I* **80**, 969 (1984).
10. Bond, G. C., and Gelsthorpe, M. R., *J. Chem. Soc. Faraday Trans. I* **85**, 3767 (1989).
11. Blankenburg, K. J., and Datye, A. K., *J. Catal.* **128**, 186 (1991).
12. Logan, A. D., and Paffett, M. T., *in* "Proceedings, 10th International Congress on Catalysis, Budapest, 1992" (L. Guczi, F. Solymosi, and P. Tetenyi, Eds.). Akadémiai Kiadó, Budapest, 1993.
13. Rodriguez-Reinoso, F., Rodriguez-Ramos, I., Moreno-Castilla, C., Guerrero-Ruiz, A., and Lopez-Gonzalez, J. D., *J. Catal.* **107**, 1 (1987).
14. Cortright, R. D., and Dumesic, J. A., *J. Catal.* **148**, 771 (1994).
15. Xu, C., Koel, B. E., and Paffett, M. T., *Langmuir* **10**, 166 (1994).
16. Mériaudeau, P., Auroux, A., and Viornery, C., submitted for publication.